Analysis of Aggregate Interference and Primary System Performance in Finite Area Cognitive Radio Networks

Luxmiram Vijayandran, *Student Member, IEEE,* Prathapasinghe Dharmawansa, *Member, IEEE,* Torbjörn Ekman, *Member, IEEE,* and Chintha Tellambura, *Fellow, IEEE*

***Abstract*—This paper considers the analytical performance of primary users (PUs) subject to interference due to secondary users (SU) in an underlay cognitive radio system over Rayleigh fading. In particular, we focus on a more general spatial configuration where the interfered PU, not only located at the center of the cell, is having a protective region which is free of SUs and the SUs are distributed over a *finite area* in contrast to the commonly used infinite area assumption. We first characterize the statistical properties of the aggregate interference at the PU due to SUs, by deriving new exact closed form expressions for the moment generating function, cumulants, first, second and third moments and first order expansions of the cumulative distribution functions corresponding to propagation scenarios with path loss factors, two and four. We then investigate the PU performance by presenting new analytical expressions for the outage probability, amount of fading as well as the diversity order and coding gain. Our results indicate that the PU can achieve the full diversity gain given a non-zero protective region around the PU.**

***Index Terms*—Aggregate interference, amount of fading (AoF), coding gain, cognitive radio (CR), cumulants, diversity order, moment generating function (MGF), outage probability.**

I. Introduction

In recent years, cognitive radio (CR) technology [1], [2] has become a popular candidate to overcome the increasing scarcity of the radio spectrum, by allowing the secondary users (SUs) to opportunistically sense and utilize the available spectrum. Two main approaches are envisioned in CR developments with the so-called underlay and overlay systems [3]. The more conservative approach of the overlay system is at a cost of lower efficiency in terms of SUs throughput. Thus, although more challenging, it is sensible to put more effort on the underlay research to foster the CR appealing paradigm.

The characterization of the interference on the target users in different network configurations is crucial for the design of efficient interference management techniques [3]. Although being a well researched topic, the CR development has brought it again into the focus of researchers. Specifically, the analysis of the aggregate interference at the PU due to the SUs has been of great recent interest (e.g., [4]–[9]). The aggregate interference in a Poisson field of interferers was first studied in [10]. The interference was shown to follow a stable distribution with infinite variance. That work has then been extended to handle more practical issues such as: various type of channel fading (e.g., [6], [7], [11]), probability distribution approximations (e.g., [4], [12], [13]), interferers using power control (e.g., [5], [12]), or sensing capabilities (e.g., [4], [8], [14]). The outage probability of the interfered nodes in different channel environments have also been investigated in e.g., [6], [7], [15]. The general approach which has hitherto been used to characterize the interference is, first to evaluate its characteristic function (CF) (see e.g., [14]), and then to apply the inverse Fourier transform to compute the probability distribution function (PDF). However, in many scenarios, the CF may only be expressed in an integral form. The alternative way, in practice is to numerically evaluate the Fourier inverse integral or use approximation methods.

Undeniably, the aforementioned works and references therein highly contribute to the development of a very general and unified framework for the interference characterization as envisioned in e.g., [14]. Yet, a significant amount of research is still required. In particular, this work aims to contribute in tackling three of those main issues. First, the analytical complexity of the expressions, in many earlier works, do not provide much insights into the statistical behavior of the aggregate interference in terms of the environmental and spatial physical parameters; Second, the interfered user can also experience a non-symmetric interference pattern; Third, and most importantly, instead of the commonly assumed *unbounded area* interferers, mainly due to mathematical tractability, we analyze the more realistic finite case. The second and the latter combined allows various practical applications as further described in the system model.

Only few works have attempted to investigate the finite

Paper approved by M. R. Beuhrer, the Editor for Cognitive Radio and UWB of the IEEE Communications Society. Manuscript received December 1, 2010; revised August 8, 2011 and January 13, 2012.

L. Vijayandran and T. Ekman are with the Department of Electronics and Telecommunications, Norwegian University of Science and Technology, Trondheim, Norway (e-mails: luxmiram.vijayandran@gmail.com; torbjorn.ekman@iet.ntnu.no).

P. Dharmawansa is with the Department of Communications and Networking, Aalto School of Electrical Engineering, Espoo, Finland (e-mail: prathapakd@ieee.org).

C. Tellambura is with the Department of Electrical Engineering, University of Alberta, Edmonton, AB T6G 2V4, Canada (e-mail: chintha@ece.ualberta.ca).

This paper was presented in part at the IEEE 22nd International Symposium on Personal, Indoor and Mobile Radio Communications, Toronto, ON, Canada, Sep. 2011.

The work of L. Vijayandran and T. Ekman was supported by the SENDORA project funded by the EU under FP7, and the CROPS2 project under the Norwegian Research Council.

Digital Object Identifier 10.1109/TCOMM.2012.051412.100739

case. In [16], the moment generating function (MGF) of the interference has been investigated, for both the Poisson point process (PPP) and the Binomial point process (BPP) distributed interferers. Yet, the expression (see [16, eq. 6]) leaves the channel as an expectation, furthermore the interfered user is only placed at the center. In [17], the nth-moments of the interference for various practical spatial configuration are investigated with finite areas. An exact expression is provided for the special case of circular annulus (i.e., as later defined, case B in Fig. 1), whereas all other settings are provided with several integration formulation. Moreover, note that the authors in [16] and [17] do not investigate the final performance of the interfered node.

Motivated by those issues, we introduce in this work a reconfigurable spatial model based on three finite radii. As further discussed in the system model, the spatial model enjoys a wide applicability such as the IEEE 802.22 scenario, and interferers with different path loss exponent (PLE). In particular, the reconfigurable spatial parameters introduce more general structure to the system model in contrast to the more frequently used cell centered PU model.

In this paper, we focus on the analytical performance of the PU due to *finite area* SUs corresponding to PLE factors 2 and 4, over Rayleigh fading. We first derive new exact expressions for the MGF, cumulants, moments as well as the first order expansions of the cumulative distribution function (CDF) of the aggregate interference. Our results show that the moments are more sensitive to the radius of the SU area for a PLE of 2 than for 4. This in turn reveals that the common infinite area assumption with high PLE indices can be reasonable in some scenarios. Based on the exact MGFs of the interference, we then investigate the performance of the PU system by deriving analytical expressions for the outage probability as well as the amount of fading (AoF). In addition, we present a comprehensive investigation of the diversity order and coding gain: the two key parameters dictating performance in the high SNR regime. Our results show that the PU can achieve the maximum diversity with the non-zero protective region in contrast to the reduced diversity without a protective region. It turns out that the infinite area assumption in general undermine the system performance for relatively low PLE. This is further confirmed by our numerical results.

This paper is organized as follows: the general system model is introduced in Section II. Section III derives the key MGF results of the aggregate interference and analyzes the related statistics. The PU performance is evaluated in Section IV and Section V concludes the paper.

II. System Model

We consider a CR system which consists of both primary and secondary networks. The primary network is composed of PU receivers located anywhere within the primary cell. The secondary network lays outside the primary cell, where the SUs are uniformly distributed. This system model is depicted in Fig. 1. We assume that both PUs and SUs use a single antenna, and their communications undergo path loss and Rayleigh fading. We omit shadowing for the sake of analytical tractability and in view of obtaining some benchmark results.

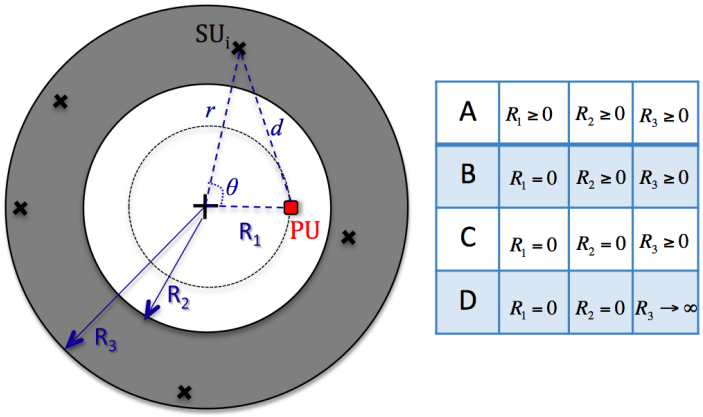

Fig. 1. System model and cases identification, defined by the three radii R_1, R_2 and R_3. The PU is symbolized by the square and the SUs by the crosses. SUs are assumed to be uniformly distributed in the finite area between R_2 and R_3 while the number of SUs are Poisson distributed.

In this paper, we aim at characterizing the statistics of the aggregate interference generated by the SUs at any given PU and subsequently evaluate its performance. Note that the PUs being located anywhere in its cell, and not only at the center, the relative spatial distribution of the interferers around the PUs is asymmetric (as in [18]), in contrast to the simple symmetric case as in most of the previous works e.g., [4]–[12], [16].

The system spatial parameters are defined by the three radii R_1, R_2 and R_3 such that $R_1 \leq R_2 < R_3$, where R_1 is the distance of the PU from the center, and R_3 is the finite radius of the secondary network. R_2 can be simply defined as the primary cell radius (R_p), but can also account for an additional guard band around the primary cell [19] (i.e., $R_2 = R_p + \epsilon, \epsilon \geq 0$). Thus, PUs are within R_p, and SUs are beyond R_2. This finite three-radii configurable network allows many practical combinations, thus enjoying wide applicability such as follows:

1) When designing a CR system, aided by a fixed deployed wireless sensor network, it is inherently of finite localized size. The interference of interest is the one produced by this new network, which can allow the design of appropriate power control policies as in [3] to fulfill the regulatory requirements.
2) One major application, when $R_1 > 0$ (i.e., the PU is not located at the center), is the IEEE 802.22 (WRAN) Digital TV (DTV) (see e.g., [18], [20]). IEEE has been developing the IEEE 802.22 standard for Wireless Regional Area Networks (WRAN), to opportunistically access the spectrum that is not currently used by the TV broadcasting stations. In a DTV scenario, a base station (BS) broadcasts the signals within a certain area to a TV receiver (i.e., R_1). The secondary system, based on the broadcast signal (beacon) strength, can estimate the distance from the primary BS which is located at the center of the system. Thus, a minimum protective circle can be enforced by regulation to the secondary system (i.e., R_2). It is clear that the previous works' model assuming symmetric interferers pattern and corresponding results cannot apply for this application.

3) It is known that as the distance increases, the PLE increases as well. One of the simplest example is the two-ray model [21] with PLE indices 2 and 4. However, previous works could only assume one PLE. Our model allows to cumulate different areas interference with different PLE (by successively varying the 3 finite radii configuration and computing the interference in each area, and finally summing up). However, while it can be exactly computed when the interfered PU is at the center, or approximately when close to the center, the cumulation of different PLE cannot be well approximated if the PU is at the edge of its cell (since the PLE-drop is PU-centric and not BS-centric).

In practical scenarios, only the statistical knowledge of the interferers location is available. Thus, following [10], we may as well treat them as completely random according to a homogeneous PPP[1] in the two dimensional plan. The probability of N SUs being inside a region depends only on the total area and follows a Poisson distribution with mean $\lambda\pi R_{32}$, given by

$$\Pr(N=n) = \exp\left(-\lambda\pi R_{32}\right)(\lambda\pi R_{32})^n/n!, \quad n \geq 0 \qquad (1)$$

where $R_{32} = (R_3^2 - R_2^2)$ and λ characterizes the SU density per unit area. The effect of multiple-tiers interferers networks [22] could be envisioned where each network is defined by different density and transmit power, but is beyond the scope of this work. Note that it is possible to consider the case where each SU only transmits with a probability ρ_{tx}, in which case the set of transmitting SUs also forms a Poisson process with a new scaled density $\lambda_2 = \lambda_1\rho_{\text{tx}}$ [10]. This elegant theory provides a tractable and practical model and has prevailed in many works e.g., [4], [6]–[8], [10]–[12], [14]. Other models have also been proposed in the literature (e.g., a BPP has been investigated in [23] to model the arrangement of the nodes when N is known, and does not assume independency of the number of nodes in disjoint areas.). In particular, with the explosion in the different type of heterogeneous networks (e.g., femtocells, hotspots, relays, meshing approaches), the need for different spatial models is essential (see [24, Table 1]).

We assume that each SU has the same transmit power P_{SU}, decays according to the path loss law, and undergoes independent and identically distributed (i.i.d.) Rayleigh fading. Thus, the aggregate interference I at the PU can be defined as

$$I = \sum_{i=1}^{N} I_i = \sum_{i=1}^{N} P_{SU} d_i^{-\alpha} \left|h_{SU_i}\right|^2, \qquad (2)$$

where I_i is the interference due to the ith SU, d_i is the distance between the PU and the ith SU, α is the PLE, and $\left|h_{SU_i}\right|^2$ is the exponentially distributed power envelope, i.e., with density function $f_{|h_{SU}|^2}(x) = (1/\Omega)\exp\left(-x/\Omega\right)$, where Ω is the mean power[2]. Without loss of generality we assume in the sequel a unit mean power, i.e., $f_{|h_{SU}|^2}(x) = \exp\left(-x\right)$. Moreover, we assume that $\left|h_{SU_i}\right|^2$ is independent of d_i.

In most practical situations, the PLE generally varies between 1.6 (e.g., hallways inside buildings) and 6 (e.g., dense urban environments) [21]. However, in this work, due to mathematical tractability, we mainly focus on the two most frequently used propagation scenarios in the literature, namely with PLE given by 2 (i.e., free space) and 4.

We consider four different practical configurations in terms of the finite radii R_1, R_2 and R_3 as summarized in the table given in Fig. 1. This spatial model is easily reconfigurable to obtain a spectrum of useful spatial structures as mentioned earlier. Case A is the most general setting which incorporates the three other cases: B, C and D. The general use of our model, depicted in Fig. 1, can be summarized as follows:

1) The IEEE 802.22 scenario with the PU being the TV receiver, as well as the classical downlink cellular network with the PU being the mobile, can be characterized by Case A with $R_1 > 0$, where the center represents the BS.
2) Case B (i.e., Case A with $R_1 = 0$), Case C, and Case D, characterize the PU centric interference analysis scenarios.

Notable configuration is Case D with $R_2 \geq 0$, which has been used to analyze the aggregated interference in most of the aforementioned works, see e.g., [6], [7], [10], [11], [15], [19], etc... Yet, our analysis still provide further new insights into the Case D, especially in terms of the PU performance measures. It is important to note that Case D is only applicable for $\alpha > 2$, since the aggregate interference tends to infinity for $\alpha \leq 2$ as $R_3 \to \infty$ [10].

III. Statistics of the Interference

In this section, we first derive exact closed-form expressions for the MGF of the aggregate interference. Subsequently, they will be employed to evaluate different statistics of I and to gain insights into the behavior of the CDF of I.

A. Moment Generating Function of I

By definition [26], the MGF of the aggregate interference I defined in (2), for a specific PLE α, is $\mathcal{M}_I^{(\alpha)}(s) = \mathbb{E}_I\left\{\exp\left(-sI\right)\right\}$. Since the number of interferers N is a poisson distributed random variable, $\mathcal{M}_I^{\alpha}(s)$ can be written as [10]

$$\begin{aligned}\mathcal{M}_I^{(\alpha)}(s) &= \mathbb{E}_N\left\{\mathbb{E}_I\left\{\exp\left(-sI\right)|N\right\}\right\} \\ &= \sum_{N=0}^{\infty} \frac{1}{N!}\mathbb{E}_I\left\{\exp\left(-sI\right)|N\right\} \\ &\qquad \times \exp\left(-\lambda\pi R_{32}\right)(\lambda\pi R_{32})^N. \qquad (3)\end{aligned}$$

[1]The spatial Poisson process is a natural choice in such situations, given that the PDF of a node position inside a region is conditionally uniform. Moreover, the Poisson process has maximum entropy among all homogeneous processes [14].

[2]Following [25, Section 4.2], it can be shown that to model the joint effect of the shadowing and Rayleigh, it is sufficient to consider the mean power of the Rayleigh envelope as a lognormal random variable, i.e., using $f_{|h_{SU}|^2}(x) = \mathbb{E}_\Omega\left\{(1/\Omega)\exp\left(-x/\Omega\right)\right\}$, where Ω follows the lognormal distribution [25, eq. 2.200].

The random variables I_i, $i = 1...N$, being i.i.d., we get

$$\mathbb{E}_I\left\{\exp\left(-sI\right)|N\right\} = \mathbb{E}_I\left\{\exp\left(-s\sum_N I_i\right)\right\} = \mathbb{E}_{I_i}\left\{\exp\left(-sI_i\right)\right\}^N = M_i^{(\alpha)}(s)^N \quad (4)$$

where $M_i^{(\alpha)}(s) = \mathbb{E}_{I_i}\left\{\exp\left(-sI_i\right)\right\}$ is the MGF of the interference due to the ith SU. Substituting (4) into (3), the aggregate interference MGF can be written as

$$\mathcal{M}_I^{(\alpha)}(s) = \exp\left(-\lambda\pi R_{32}\right)\sum_{N=0}^{\infty}\frac{1}{N!}(M_i^{(\alpha)}(s)\lambda\pi R_{32})^N = \exp\left(\lambda\pi R_{32}\left(M_i^{(\alpha)}(s)-1\right)\right). \quad (5)$$

Since $M_i^{(\alpha)}$, the MGF of the ith interferer, is independent of i, in what follows, without loss of generality, we omit the index i. In our model, the randomness of each individual interference stems from two factors, the random distance (i.e., d), and the fading power envelope (i.e., $|h_{SU}|^2$). In the sequel, it is mathematically more convenient to use the polar coordinates (r, θ) instead of d, as defined in Fig. 1. Thus, we employ the following geometric relation

$$d(r,\theta) = \sqrt{r^2 + R_1^2 - 2rR_1\cos\theta}. \quad (6)$$

As such, the individual interference MGF can be written as

$$M^{(\alpha)}(s) = \mathbb{E}_{r,\theta}\left\{\int_0^{\infty}\exp\left(-sP_{SU}d^{-\alpha}(r,\theta)x\right)f_{|h_{SU}|^2}(x)dx\right\} \quad (7)$$

where the expectation is taken with respect to r and θ. Now, the inner integral in (7) can be solved using the MGF of $|h_{SU}|^2$ to yield

$$M^{(\alpha)}(s) = \mathbb{E}_{r,\theta}\left\{\frac{1}{1+sP_{SU}d^{-\alpha}(r,\theta)}\right\}. \quad (8)$$

Note that the convergence of Laplace transform is satisfied if $\Re(s)P_{SU} > -d^{\alpha}(r,\theta)$. Thus, we can as well assume in the sequel that $\Re(s) > 0$, since it always satisfies the inequality. It is important for the expectation evaluation in (8) to carefully define the spatial distribution of the interferers in terms of r and θ. Since SUs are uniformly distributed in a circular area, the larger is r, the larger is the perimeter, and also more probable is the presence of a SU at a greater distance r. Therefore, the PDF of r is given by the ratio of perimeter over area as [10], $f_R(r) = 2r/R_{32}$ for $r \in [R_2, R_3]$, and the angular distribution is uniformly distributed over $[0, 2\pi)$ i.e., $f_\theta(\theta) = 1/2\pi$. Using (6) and the PDF or r and θ, (8) can be written as

$$M^{(\alpha)}(s) = \frac{1}{\pi R_{32}}\int_{R_2}^{R_3} r g^{(\alpha)}(r)\,dr \quad (9)$$

where

$$g^{(\alpha)}(r) = \int_0^{2\pi}\frac{d\theta}{1+sP_{SU}\left(r^2+R_1^2-2rR_1\cos\theta\right)^{-\alpha/2}}. \quad (10)$$

Finally, evaluating (9) and substituting back results into (5) gives the exact closed-form expression of $\mathcal{M}_I^{(\alpha)}(s)$. However, the evaluation of (10) for an arbitrary value of α seems an arduous task. Therefore, we confine ourselves to some particular values of α. The following propositions characterize $\mathcal{M}_I^{(\alpha)}(s)$ for the special representative cases, $\alpha = 2$ and $\alpha = 4$.

Proposition 1: The MGF of the aggregate interference at the PU, for $\alpha = 2$, is given by

$$\mathcal{M}_I^{(2)}(s) = \exp\left(-sP_{SU}\lambda\pi\ln\Psi^{(2)}(s)\right) \quad (11)$$

where

$$\Psi^{(2)}(s) = \begin{cases} \frac{\sqrt{4sP_{SU}R_1^2+(R_3^2-R_1^2+sP_{SU})^2}+(R_3^2-R_1^2+sP_{SU})}{\sqrt{4sP_{SU}R_1^2+(R_2^2-R_1^2+sP_{SU})^2}+(R_2^2-R_1^2+sP_{SU})} & \text{Case A} \\ \frac{R_3^2+sP_{SU}}{R_2^2+sP_{SU}} & \text{Case B} \\ \frac{R_3^2+sP_{SU}}{sP_{SU}} & \text{Case C.} \end{cases}$$

Proof: See Appendix A-A. ■

Proposition 2: The MGF of the aggregate interference at the PU, for $\alpha = 4$, is given by

$$\mathcal{M}_I^{(4)}(s) = \exp\left(-\sqrt{sP_{SU}}\lambda\pi\Psi^{(4)}(s)\right) \quad (12)$$

where

$$\Psi^{(4)}(s) = \begin{cases} \arctan\left(\frac{\sqrt{sP_{SU}}\left(R_3^2-R_2^2\right)}{R_3^2R_2^2+sP_{SU}}\right) & \text{Case B}^3 \\ \arctan\left(\frac{R_3^2}{\sqrt{sP_{SU}}}\right) & \text{Case C} \\ \pi/2 & \text{Case D.} \end{cases}$$

Proof: See Appendix A-B. ■

One can note that the special scenario $\alpha = 4$ Case D which has been analyzed in most of the previous works (e.g., [6], [7], [10], [15], [19], and in particular e.g., [11]), gives a simple analytical expression. Moreover, the general Case A for $\alpha = 4$ seems mathematically intractable (see Appendix A-B). Therefore, in what follows we only focus on the scenarios given in Propositions 1 and 2. In the sequel, for brevity, we will denote, for example the MGF corresponding to the scenario $\alpha = 2$ Case A as $\mathcal{M}_I^{(2,A)}(s)$.

B. Cumulants of I

By invoking the central limit theorem (CLT), one may tempt to approximate the PDF of I with a Gaussian PDF. However simulations have shown (e.g., see[4]) that the PDF is positively skewed and thus deviates from normality. This stems from the fact that interferers very close to the receiver terminal contribute a disproportionately large amount of interference, thus limiting the applicability of the central limit theorem. Therefore, the important basic parameters to approximate I are the mean, the variance, as well as the skewness. We now evaluate those statistics using the cumulants of I. By definition, the nth cumulant of I is given by [26]

$$\kappa_n^{(\alpha)} = (-1)^n\frac{d^n}{ds^n}\ln\mathcal{M}_I^{(\alpha)}(s)\Big|_{s=0}.$$

[3]Alternatively, $\arctan\left(\left(\sqrt{sP_{SU}}\left(R_3^2-R_2^2\right)\right)/\left(R_3^2R_2^2+sP_{SU}\right)\right) = \arctan\left(R_3^2/\sqrt{sP_{SU}}\right) - \arctan\left(R_2^2/\sqrt{sP_{SU}}\right)$.

The first three cumulants are related to the mean, variance, and skewness respectively through the relations [26],

$$\mu_I^{(\alpha)} = \kappa_1^{(\alpha)}$$
$$\sigma_I^{(\alpha)2} = \kappa_2^{(\alpha)}$$
$$\delta_I^{(\alpha)} = \mathbb{E}_I\left\{\exp\left(\frac{I-\mu_I}{\sigma_I}\right)^3\right\} = \frac{\kappa_3^{(\alpha)}}{\kappa_2^{(\alpha)3/2}}.$$

Using (11) in (III-B) followed by the repetitive application of L'Hôpital rule with some lengthy algebraic manipulation yield the 1st, 2nd and 3rd cumulants corresponding to the scenario $\alpha = 2$, Case A with $R_1 \neq R_2$ as

$$\kappa_1^{(2,A)} = \lambda\pi P_{SU} \ln\left(\frac{R_3^2 - R_1^2}{R_2^2 - R_1^2}\right)$$
$$\kappa_2^{(2,A)} = \frac{2\lambda\pi P_{SU}^2 \left\{R_3^4 R_2^2 - R_2^4 R_3^2 + R_1^4 R_2^2 - R_1^4 R_3^2\right\}}{\left(R_2^2 - R_1^2\right)^2 \left(R_3^2 - R_1^2\right)^2}$$
$$\kappa_3^{(2,A)} = \frac{3\lambda\pi P_{SU}^3 g(R_1, R_2, R_3)}{\left(R_2^2 - R_1^2\right)^4 \left(R_3^2 - R_1^2\right)^4}$$

where

$$\begin{aligned} g(R_1, R_2, R_3) = {} & 2R_2^2 R_1^2 \left(R_3^2 - R_1^2\right)^4 - 2R_3^2 R_1^2 \left(R_2^2 - R_1^2\right)^4 \\ & + 2R_2^2 R_3^2 \left(R_2^2 - R_1^2\right)^2 \left(R_3^2 - R_1^2\right)^2 - 2R_3^4 \\ & \left(R_2^2 - R_1^2\right)^4 + R_2^4 R_3^4 \left(R_3^2 - R_2^2\right)^2 - 2R_1^4 R_2^2 \\ & R_3^2 \left(R_3^2 - R_2^2\right)^2 + R_1^8 \left(R_3^2 - R_2^2\right)^2. \end{aligned}$$

Similar calculations yield the first three cumulants corresponding to $\alpha = 4$, Case B with $R_2 > 0$ as

$$\begin{aligned} \kappa_1^{(4,B)} &= \lambda\pi P_{SU}\left(\frac{1}{R_2^2} - \frac{1}{R_3^2}\right) \\ \kappa_2^{(4,B)} &= \frac{2}{3}\lambda\pi P_{SU}^2\left(\frac{1}{R_2^6} - \frac{1}{R_3^6}\right) \\ \kappa_3^{(4,B)} &= \frac{6}{5}\lambda\pi P_{SU}^3\left(\frac{1}{R_2^{10}} - \frac{1}{R_3^{10}}\right) \end{aligned} \tag{13}$$

which are consistent with the general cumulant equation given in [15, eq. 13] for $\alpha > 2$ Case B and without considering any fading. It is interesting to observe that including the Rayleigh fading simply scale the cumulants compared to the case without fading (i.e., compare (13) with [15, eq. 13]). Similar observations have been made in [11] when comparing the PDF/CDF [11, eq. 8] with and without Rayleigh fading.

The three cumulants can be used to approximate the PDF of I, with limited accuracy, using e.g., Edgeworth expansion or the shifted log-normal approximations [4]. Furthermore, these remarkably simple expressions show us how the interference statistics change with different physical parameters. A careful inspection of these expressions reveal that the importance of having the guard radius (i.e., $R_2 > 0$) around the PU. As such, this protected region controls the severity of the interference experienced by the PU, thereby stabilizing the PU performance as we will see in due course. Moreover, the propagation scenario corresponding to $\alpha = 4$ induces less interference to the PU in comparison with the scenario corresponding to $\alpha = 2$, on the average. Interestingly, the identical re-scaling of the spatial parameters (i.e., when R_1, R_2, R_3 are replaced, for $k > 0$, with kR_1, kR_2, kR_3, respectively) does not affect the mean of I corresponding to $\alpha = 2$. However, it affects the statistics of $\alpha = 4$ case.

Note that the cumulants in Case C or Case D are intractable as the corresponding values of mean and variance tend to infinity. This is consistent with the comments already made in e.g., [6], [10], where the interference has been shown to approach a alpha-stable distribution (or Lévy distribution), when the the protective region tends to zero (i.e., CLT cannot be applied). In that situation the path loss model defined in (2) has a singularity [27] at $d = 0$ and is generally not valid for $d < 1$, as the wireless channel can not amplify the transmitted signal. In this type of scenario, stable distributions have unbounded (infinite) second-order moment due to that singularity. In [28], a truncated-stable distribution has been very recently proposed for smooth tails and finite moments, offering an alternative statistical tool to model the aggregate interference in more realistic scenarios without this singularity. Based on $\kappa_1^{(2,A)}$, if R_2 and R_3 are fixed and R_1 (i.e., PU) varies from the center of the cell to the edge, the interference mean increases much faster than with a linear trend. Therefore, one can expect the average performance of the primary cellular network to be much better inside than at the edge of the primary cell, which is also intuitively correct. Since $\kappa_1^{(2)} \to \infty$ while $\kappa_1^{(4,B)}$ remains finite as $R_3 \to \infty$, we can analytically verify the similar claim given in [10] as an observation. Moreover, in [4], general semi-analytical expressions are provided to compute the nth cumulant for Case D with $R_2 = 1$, $\forall \alpha > 2$. Although they are based on different channels and sensing techniques, those integral expressions do not provide simple direct insights and are not valid for scenarios such as Case A or Case B.

Figs. 2(a) and 2(b) compare the mean, the variance and the skewness between the analytical results and corresponding Monte-Carlo simulations averaged over 10^5 random simulations. As can be seen from the figure, the first two moments of the aggregate interference is more resilient to the variation of R_3 for PLE index $\alpha = 4$ than $\alpha = 2$.

C. Probability Distributions

To evaluate the PDF of the aggregate interference, a natural method is to directly invert its MGF using the standard Laplace inversion techniques. This approach, however, appears intractable for general system configurations due to the complexity of the MGF expressions (11) and (12). Nevertheless, for the special case $\alpha = 4$ Case D, the inverse Laplace of $\mathcal{M}_I^{(4,D)}(s) = \exp\left(-\sqrt{s}\sqrt{P_{SU}}\lambda\pi^2/2\right)$ can be found using [29, eq. 2.2.1.9] to obtain the PDF and CDF of I already given in [11, eq. 8]. Yet, it is important to note that infinite series solutions for the probability distributions can be obtained for general cases using the power series expansion method of Laplace inversion given in [30, Chap. 4.2]. The main drawback of this approach in practice is that such infinite series do not converge rapidly and thus require a large number of terms for numerical evaluations. Among other methods, there exists a numerical Fourier inversion method based on the characteristic function of I [31, eq. 3.6].

A useful alternative approach is to characterize the CDF of I around the origin which is of paramount importance in analyzing the performance of general CR systems. Thus, in

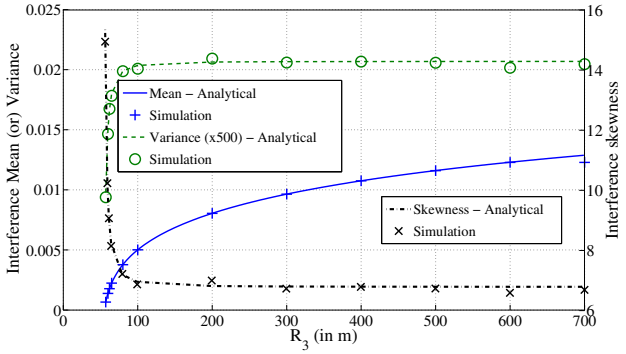

(a) $\alpha = 2$, $R_1 = 50$m and $R_2 = 55$m.

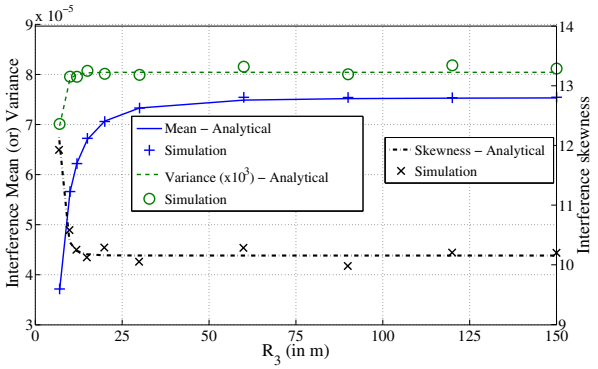

(b) $\alpha = 4$, $R_1 = 0$m and $R_2 = 5$m.

Fig. 2. Illustration of the effect of R_1, R_2 and R_3 on the mean, variance and skewness of the aggregate interference. Results are shown for $\lambda = 10^{-4}$ and $P_{SU} = 30$dBm.

what follows we focus on obtaining the first order expansions of the CDFs of I corresponding to $\alpha = 2$ and $\alpha = 4$, for Case A and Case B, respectively. To this end, we utilize the initial value theorem along with the MGF of I. As such, for a function $f(t)$ having Laplace transform $\mathcal{F}(s)$, the initial value theorem states $\lim_{t\to 0} f(t) = \lim_{s\to\infty} s\mathcal{F}(s)$. Before proceeding, let us define the CDF of I as $F_I^{(\alpha)}(z)$ which in turn gives the Laplace transform $\mathcal{M}_I^{(\alpha)}(s)/s$. Now, invoking the initial value theorem yields

$$\lim_{z\to 0} F_I^{(\alpha)}(z) = \lim_{s\to\infty} s\frac{\mathcal{M}_I^{(\alpha)}(s)}{s} = \lim_{s\to\infty} \mathcal{M}_I^{(\alpha)}(s). \quad (14)$$

It turns out that the behavior of the CDF of I around the origin is governed by the behavior of the MGF of I at infinity. Therefore, we consider the expansion of $\mathcal{M}_I^{(\alpha)}(1/z)$ around $z = 0$, where $z = 1/s$. The following proposition characterizes the behavior of the CDF of I pertaining to $\alpha = 2, 4$ at the origin.

Proposition 3: The first order expansions of the CDFs of I corresponding to $\alpha = 2$ Case A and $\alpha = 4$ Case B with *finite* R_3 are respectively given by

$$F_I^{(2,A)}(z) \approx \exp\left(-\lambda\pi R_{32}\right) + \exp\left(-\lambda\pi R_{32}\right) \frac{\lambda\pi\left(\left(R_3^4 - R_2^4\right) + 2R_1^2 R_{32}\right)}{2P_{SU}} z, \quad (15)$$

$$F_I^{(4,B)}(z) \approx \exp\left(-\lambda\pi R_{32}\right) + \exp\left(-\lambda\pi R_{32}\right)$$

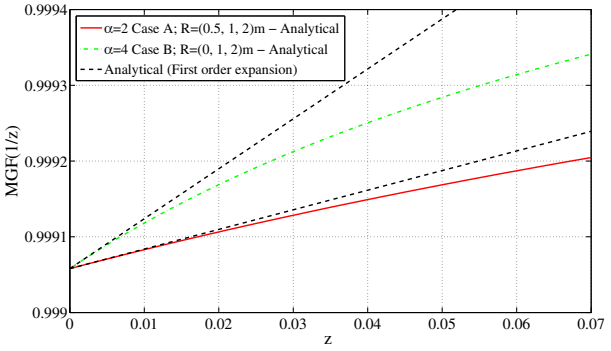

Fig. 3. Comparison of the exact and first order expansion approximation of $\mathcal{M}_I(1/z)$ around $z = 0$. The constant parameters are: $\lambda = 10^{-4}$ and $P_{SU} = 30$dBm.

$$\times \frac{\lambda\pi\left(R_3^6 - R_2^6\right)}{3P_{SU}} z. \quad (16)$$

Proof: See Appendix B. ■

Remark: It should be noted that $\alpha = 4$ Case D has been excluded from Proposition 3. Clearly, under this scenario (i.e., when $R_3 \to \infty$), the infinite series expansion (39) converges only at the point $z = 0$. Therefore, we cannot simply set $R_3 \to \infty$ in (15) to characterize $F_I^{(4,B)}(z)$ in the vicinity of the origin.

The results in Proposition 3 reveal that there exists a non-zero finite probability of having zero interference (i.e., $F_I(0) = \exp\left(-\lambda\pi R_{32}\right)$) at the PU in a finite area cognitive network for $\alpha = 2$ and 4. This behavior of I has been unobserved in the previous works, since the infinite R_3 assumption in turn gives $F_I(0) = 0$. As such, for finite R_3, the PDF of I contains a discrete probability mass at the origin, which is usually represented with a Dirac delta function. This behavior stems from the fact that the number of SUs, N, is randomly distributed according to the Poisson process (1). Thus, there is a non-zero probability that $N = 0$, which intuitively increases as the area becomes smaller, corroborating with $F_I(0) = \exp\left(-\lambda\pi R_{32}\right)$. Obviously, this probability drops rapidly in terms of radius because of the negative exponential. Nevertheless, it is useful to know that the probability is not simply zero. This behavior can be of paramount importance in interference management, especially in small size systems.

Fig. 3 illustrates the accuracy of Proposition 3 for both $\alpha = 2$ Case A and $\alpha = 4$ Case B with $\lambda = 10^{-4}$. Moreover, the interferes radii are set to $R_2 = 1$m and $R_3 = 2$m respectively. Clearly, the linear behavior of $\mathcal{M}_I(1/z)$ around the origin perfectly matches with the results given by Proposition 3.

Having armed with the various statistical parameters of I, let us now focus in analyzing the PU performance in a finite area cognitive network.

IV. PU System Performance

Here we investigate the performance of the primary system based on the MGF developed in the previous section.

A. Outage Probability (P_{out})

The outage probability is an important measure in determining the quality of service. It is defined as the probability

that the instantaneous received SINR (signal-to-interference-noise-ratio) γ drops below a threshold γ_{th} i.e., $P_{\text{out}}(\gamma_{\text{th}}) = \Pr(\gamma \leq \gamma_{\text{th}})$. Also, by definition $P_{\text{out}}(\gamma_{\text{th}}) = F_{\gamma}(\gamma_{\text{th}})$ where $F_{\gamma}(\gamma_{\text{th}})$ is the CDF of γ. The average received power at the PU is defined as P_{PU}. Thus, assuming unit variance noise[4] at the PU, the instantaneous SINR at the PU can be written as

$$\gamma_{PU} = \frac{P_{PU}\left|h_{PU}\right|^2}{I+1} \tag{17}$$

where I is the aggregate interference due to SUs as defined in (2) and $\left|h_{PU}\right|^2$ is the exponentially distributed power envelope with unit mean. Furthermore, it is reasonable to assume that $\left|h_{PU}\right|^2$ and I are independent. Based on these assumptions, $P_{\text{out}}^{(\alpha)}(\gamma_{\text{th}})$ can be written as

$$\begin{aligned} P_{\text{out}}^{(\alpha)}(\gamma_{\text{th}}) =& \mathbb{E}_I\left\{\Pr\left(\left|h_{PU}\right|^2 \leq \frac{\gamma_{\text{th}}(I+1)}{P_{PU}}\middle| I\right)\right\} \\ =& \mathbb{E}_I\left\{F_{\left|h_{PU}\right|^2}\left(\frac{\gamma_{\text{th}}(I+1)}{P_{PU}}\right)\right\} \end{aligned} \tag{18}$$

where the CDF of $\left|h_{PU}\right|^2$ is $F_{\left|h_{PU}\right|^2}(x) = 1-\exp(-x)$. Finally, (18) can be written as

$$\begin{aligned} P_{\text{out}}^{(\alpha)}(\gamma_{\text{th}}) &= \mathbb{E}_I\left\{1-\exp\left(-\frac{\gamma_{\text{th}}(I+1)}{P_{PU}}\right)\right\} \\ &= 1-\exp\left(-\frac{\gamma_{\text{th}}}{P_{PU}}\right)\mathcal{M}_I^{(\alpha)}\left(\frac{\gamma_{\text{th}}}{P_{PU}}\right). \end{aligned} \tag{19}$$

It is interesting to note that the primary user outage probability is explicitly governed by the MGF of the aggregate interference. Since $\mathcal{M}_I^{(\alpha)}\left(\frac{\gamma_{\text{th}}}{P_{PU}}\right) \leq 1$ for $\gamma_{\text{th}} \geq 0$, a simple calculation gives

$$P_{\text{out}}^{(\alpha)}(\gamma_{\text{th}}) \geq 1-\exp\left(-\frac{\gamma_{\text{th}}}{P_{PU}}\right).$$

This in turn reveals that the interference due to SUs degrades the outage of the PU.

Fig. 4(a) compares the outage probability between the analytical (i.e., (19) with (11) and (12)) and simulated Monte-Carlo results with several settings for both $\alpha = 2$ and $\alpha = 4$. As can be seen from the figure, the impact of the secondary network radius (i.e., R_3) on the outage of the PU is more significant for $\alpha = 2$ than $\alpha = 4$. In the light of this observation, we can conclude that the theoretically infinite assumption for R_3 can be a reasonable approximation for propagation scenarios with relatively high PLE. Fig. 4(b) illustrates the effect of the PLE on the outage of the PU. The outage curves corresponding to the PLE indices $1.5, 3, 4$ and 6 are obtained by numerically evaluating (9) with (5) and (19). It is easy to note that beyond $\alpha = 4$, the outage results for higher exponents are nearly similar. This in turn reveal that the analytical results in the case of $\alpha = 4$ can be considered as good approximations to the propagation scenarios corresponding to the PLE indices higher than 4. Note that if one consider the additional shadowing effect, the investigations performed in e.g., [6], [7], [15], have shown that increasing the standard deviation of the shadowing deteriorates the outage probability at the PU. Thus, the results obtained here, considering only Rayleigh fading, could provide a benchmark, i.e, a minimum P_{out} to be expected.

[4]For the sake of generality we do no omit the noise, since by increasing the guard band (i.e., R_2), the system will shift from an interference-limited to the classical noise-limited environment. Note that scaling the noise simply implies rescaling the powers, P_{PU}, and P_{SU} in (2).

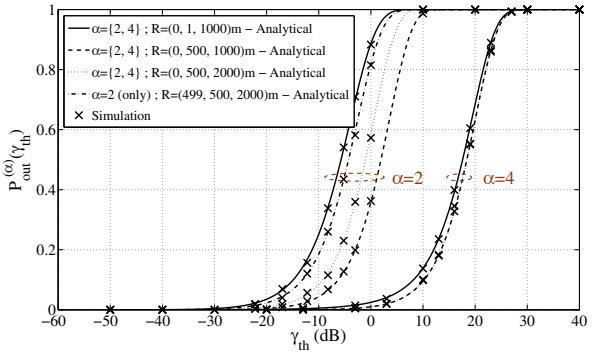

(a) $\alpha = 2$ and $\alpha = 4$ with different settings of $R = (R_1, R_2, R_3)$.

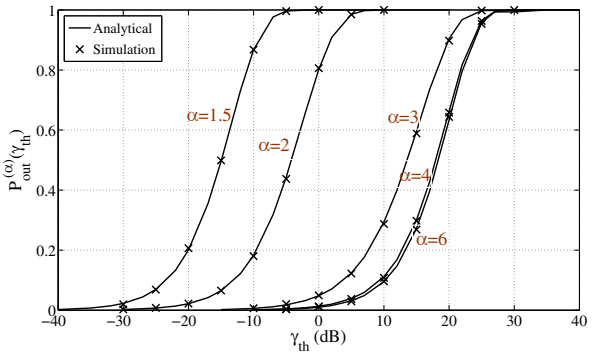

(b) Impact of α on the outage of the PU; $R = (20, 25, 500)$m.

Fig. 4. Illustration of the outage probability. The constant parameters are: $\lambda = 10^{-4}$, $N_0 = 1$, $P_{PU} = 50$dBm and $P_{SU} = 80$dBm.

B. Amount of Fading (AoF)

The AoF at the PU is an important performance measure which quantifies the severity of the fading channel. By definition, it is expressed as [32]

$$\text{AoF} = \left(m_2 - m_1^2\right)/m_1^2 \tag{20}$$

where m_1 and m_2 are the first and second moments of γ_{PU}, respectively. Now the 1st moment can be written as

$$\begin{aligned} m_1^{(\alpha)} =& \mathbb{E}_{\gamma_{PU}}\{\gamma_{PU}\} = \mathbb{E}_I\left\{\mathbb{E}_{\left|h_{PU}\right|^2}\{\gamma_{PU}\}\right\} \\ =& P_{PU}\mathbb{E}_{\left|h_{PU}\right|^2}\left\{\left|h_{PU}\right|^2\right\}\mathbb{E}_I\left\{\frac{1}{I+1}\right\}. \end{aligned} \tag{21}$$

The next challenge is to evaluate the expected value in (21). To this end, we use the following representation

$$\frac{\Gamma(p)}{x^p} = \int_0^{\infty} v^{p-1}\exp(-xv)\,dv, \quad p>0, x>0 \tag{22}$$

with $p = 1$ in (21) to yield

$$m_1^{(\alpha)} = P_{PU}\int_0^{\infty}\exp(-v)\mathcal{M}_I^{(\alpha)}(v)dv. \tag{23}$$

Although this integral seems analytically intractable for the most general MGFs, a simple closed form solution can be

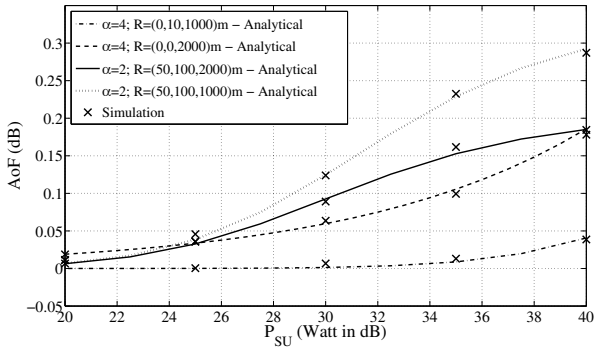

Fig. 5. Illustration of the AoF performance. The constant parameters are: $\lambda = 10^{-4}$, $N_0 = 1$ and $P_{PU} = 50$dBm.

obtained for the special case $\alpha = 4$ Case D. Under this scenario, using [33, eq. 3.462], we can obtain the exact closed-form expression

$$m_1^{(4,D)} = P_{PU}\left(1 - \left(\frac{\zeta}{\sqrt{2}}\right)\exp\left(\frac{\zeta^2}{4}\right)\sqrt{\frac{\pi}{2}}\,\mathrm{erfc}\left(\frac{\zeta}{2}\right)\right) \tag{24}$$

where $\zeta = \sqrt{P_{SU}}\lambda\pi^2/2$, and the complementary error function is defined as $\mathrm{erfc}(x) = 1 - \mathrm{erf}(x) = 1 - (2/\sqrt{\pi})\int_0^x \exp(-t^2)dt$. Following a similar approach, the 2nd moment can be written as

$$\begin{aligned} m_2^{(\alpha)} &= \mathbb{E}_{\gamma_{PU}}\left\{\gamma_{PU}^2\right\} \\ &= 2P_{PU}^2\int_0^\infty v\exp(-v)\mathcal{M}_I^{(\alpha)}(v)dv. \end{aligned} \tag{25}$$

Using again [33, eq. 3.462], this integral can be solved in closed form in the special scenario $\alpha = 4$ Case D as follows

$$m_2^{(4,D)} = 6P_{PU}^2\exp\left(\frac{\zeta^2}{8}\right)\mathcal{D}_{-4}\left(\frac{\zeta}{\sqrt{2}}\right) \tag{26}$$

where $\mathcal{D}_p(z)$ is the parabolic cylinder function. Moreover, using the three term recurrence relation (see e.g., [34, eq. 10])

$$\mathcal{D}_{-(p+1)}(z) = \frac{\mathcal{D}_{-(p-1)}(z) - z\mathcal{D}_{-p}(z)}{p} \tag{27}$$

with $\mathcal{D}_0(z) = \exp\left(-z^2/4\right)$ and $\mathcal{D}_{-1}(z) = \exp\left(z^2/4\right)\sqrt{\pi/2}\,\mathrm{erfc}\left(z/\sqrt{2}\right)$, $\mathcal{D}_{-4}(\zeta/\sqrt{2})$ can be expressed as

$$\begin{aligned} \mathcal{D}_{-4}\left(\frac{\zeta}{\sqrt{2}}\right) =& \frac{1}{3}\exp\left(-\frac{\zeta^2}{8}\right)\left(1+\frac{\zeta^2}{4}\right) \\ &- \frac{\sqrt{\pi}}{12}\zeta\exp\left(\frac{\zeta^2}{8}\right)\mathrm{erfc}\left(\frac{\zeta}{2}\right)\left(3+\frac{\zeta^2}{2}\right). \end{aligned}$$

Finally, using (23) and (25) (for $\alpha = 4$ Case D, (26) instead), the AoF in (20) can be obtained.

Fig. 5 compares the analytical curves and Monte-Carlo simulated curves for AoF performance. The analytical curve for $\alpha = 4$ Case D is obtained from the closed-form expressions based on (24) and (26), whereas $\alpha = 2$ Case A and $\alpha = 4$ Case B are obtained by numerical evaluation of (23) and (25), respectively. We can see that the effective channel of the PU is more resilient to the variations in the SU power levels for $\alpha = 4$ than $\alpha = 2$. This effective channel hardening has already been observed related to the outage probability of the PU.

C. Diversity Order, Coding Gain and Asymptotic Behavior

It has been shown in [35] that for high SNR, the symbol error probability (SEP) and the outage probability are dictated by two key parameters: the diversity order and the coding gain. The diversity order, G_d, determines the slope of the SEP versus average SNR curve, at high SNR, in a log-log scale. On the other hand, the coding gain, G_c (in decibels), determines the shift of the curve in SNR relative to a benchmark SEP curve. In particular, under mild conditions and using polynomial approximations, the SEP for high SNR can be expressed as $P_E \approx (G_c\bar{\gamma})^{-(G_d)}$, where $\bar{\gamma}$ is the average SNR. Similarly, P_{out} can also be expressed as [35]

$$P_{\mathrm{out}}(\bar{\gamma}) \approx (O_c\bar{\gamma})^{-(O_d)} \tag{28}$$

where O_d is called the outage diversity order such that $O_d = G_d$ and O_c is the coding gain which differ by a constant (in decibel) with G_c. In what follows, we only focus on the modeling of $P_{\mathrm{out}}^{(\alpha)}(\gamma_{\mathrm{th}})$ as described in [35]. Before proceeding, let us define $\bar{\gamma} = P_{PU}$ and $\rho = \gamma_{\mathrm{th}}/\bar{\gamma}$. Now the following proposition gives the diversity order and coding gain (array gain) of the PU.

Proposition 4*:* The diversity order and coding gain of the PU corresponding to $\alpha = 2$ Case A and $\alpha = 4$ Case B, D are, respectively, given by

$$\begin{aligned} O_d^{(2,A)} &= 1, \\ O_c^{(2,A)} &= \frac{1}{\gamma_{\mathrm{th}}}\left(1 - P_{SU}\lambda\pi\ln\left(\frac{R_2^2 - R_1^2}{R_3^2 - R_1^2}\right)\right)^{-1}, \quad R_1 \neq R_2, \\ O_d^{(4,B)} &= 1, \\ O_c^{(4,B)} &= \frac{1}{\gamma_{\mathrm{th}}}\left(1 + P_{SU}\lambda\pi\left(\frac{1}{R_2^2} - \frac{1}{R_3^2}\right)\right)^{-1}, \quad R_2 > 0, \\ O_d^{(4,D)} &= \frac{1}{2}, \\ O_c^{(4,D)} &= \frac{1}{\gamma_{\mathrm{th}}}\left(\frac{\sqrt{P_{SU}}\lambda\pi^2}{2}\right)^{-2}. \end{aligned} \tag{29}$$

Proof: Our objective is to obtain an expansion for $P_{\mathrm{out}}^{(\alpha)}(\rho)$ around $\rho = 0$ in the form

$$P_{\mathrm{out}}^{(\alpha)}(\rho) \approx \frac{a}{t+1}\rho^{t+1} \tag{30}$$

so that O_d and O_c in (28) are given, respectively, by $O_d = t+1$ and $O_c = \frac{1}{\gamma_{\mathrm{th}}}\left(\frac{a}{t+1}\right)^{-\frac{1}{t+1}}$.

First let us consider the detailed derivation corresponding to $\alpha = 2$ Case A, since $\alpha = 4$ Case B follows similarly. Rewrite $P_{\mathrm{out}}^{(\alpha)}(\gamma_{\mathrm{th}})$ in (19) for $\alpha = 2$ Case A as

$$\begin{aligned} &P_{\mathrm{out}}^{(2,A)}(\rho) \\ &\quad = 1 - \exp(-\rho) \\ &\qquad \times \left(\frac{\sqrt{4\rho P_{SU}R_1^2 + \xi^2(R_2,\rho)} + \xi(R_2,\rho)}{\sqrt{4\rho P_{SU}R_1^2 + \xi^2(R_3,\rho)} + \xi(R_3\rho)}\right)^{P_{SU}\lambda\pi\rho} \end{aligned}$$

where $\xi(x,\rho) = x^2 - R_1^2 + \rho P_{SU}$. Now we use the Taylor

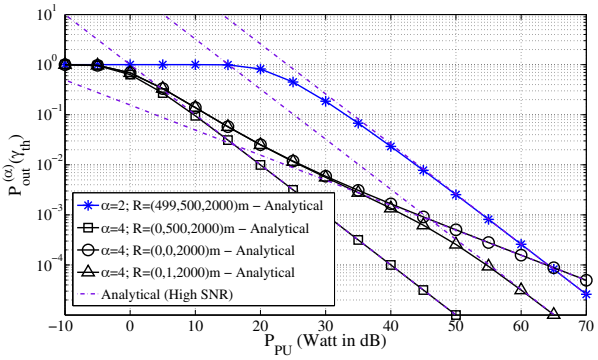

Fig. 6. Comparison of the analytical and asymptotic approximation of $P_{\text{out}}^{(\alpha)}(\gamma_{\text{th}})$ using coding gain and diversity order parameterization. Results are shown for $\gamma_{\text{th}} = 0$dB, $\lambda = 10^{-4}$, $N_0 = 1$ and $P_{SU} = 80$dBm.

expansion of $P_{\text{out}}^{(\alpha)}(\rho)$ at $\rho = 0$ to obtain

$$P_{\text{out}}^{(2,A)}(\rho) \approx 1 - \left[1 + \left(-1 + P_{SU}\lambda\pi \ln\left(\frac{R_2^2 - R_1^2}{R_3^2 - R_1^2}\right)\right)\rho\right] = \left(1 - P_{SU}\lambda\pi \ln\left(\frac{R_2^2 - R_1^2}{R_3^2 - R_1^2}\right)\right)\rho$$

which in turn gives the values corresponding to $O_d^{(2,A)}$ and $O_c^{(2,A)}$ in (29). Clearly, the above expansion, is valid only if $R_1 \neq R_2$. This is because $P_{\text{out}}^{(2,A)}(\rho)$ is not analytic at the origin for $R_1 = R_2$. Therefore, we cannot analytically quantify the diversity order and coding gain in that particular scenario.

It turns out that the order of the first non-zero term of the power series expansion of $P_{\text{out}}^{(4,D)}(\rho) = 1 - \exp(-\rho - 0.5\lambda\pi^2\sqrt{\rho P_{SU}})$ around $\rho = 0$ is $1/2$. The corresponding results $O_d^{(4,D)}$ and $O_c^{(4,D)}$ now follows from the power series expansion. ■

Interestingly, with non-zero protective region, the PU can achieve the full diversity even with $R_3 \to \infty$. However, compared to finite area interferers, the achievable diversity in the case of infinite area assumption with zero protective region is reduced by a factor of half. This reduction in the achievable diversity, which is a clear consequence of having unprotected PU, is overlooked in all previous studies.

Fig. 6 compares the exact theoretical outage probability given in (19) with the polynomial approximation given by (28). At high SINR, the asymptotic approximations clearly match with the exact outage probability curves, thereby verifying our claim.

V. Conclusions

This paper has investigated the performance of a primary user subject to Poisson distributed secondary user interferers in a CR underlay system. In contrast to infinite interferers area assumption in most of the previous studies, we have analyzed a more realistic finite interferers area. Moreover, the system model with configurable radii and the protective area around the PU enjoys a wide applicability. By employing the powerful MGF approach, first we have investigated the statistical properties of the aggregate interference at the PU due to SUs distributed in a finite area with PLE $\alpha = 2$ and $\alpha = 4$. In particular, we have presented new closed form expressions for the MGF, first three cumulants, first and second moments and first order expansions of the CDF. The statistical properties reveal that the statistical moments are more sensitive to the SU area radius in the propagation scenario corresponding to $\alpha = 2$ than $\alpha = 4$. We have subsequently applied the MGF to derive the performance of the PU in terms of the outage probability and AoF as well as the diversity and coding gains. It turns out that the theoretical infinite interferers area assumption serves as a reasonable approximation in many scenarios involving higher PLE indices.

Appendix A
Proof of Propositions 1 and 2

A. Proof of Proposition 1

Following (9), the MGF corresponding to $\alpha = 2$ can be written as

$$M^{(2)}(s) = \frac{1}{\pi R_{32}} \int_{R_2}^{R_3} r g^{(2)}(r)\, dr \tag{31}$$

where

$$g^{(2)}(r) = 2\pi - 2sP_{SU} \int_0^{\pi} \frac{d\theta}{r^2 + R_1^2 - 2rR_1\cos\theta + sP_{SU}}.$$

Using the transformation $v = \tan(\theta/2)$ and [33, eq. 2.172.c] we have

$$g^{(2)}(r) = 2\pi - \frac{2\pi sP_{SU}}{\sqrt{(R_1 + r)^2 + sP_{SU}}} \times \frac{1}{\sqrt{(R_1 - r)^2 + sP_{SU}}}. \tag{32}$$

Substituting (32) back into (31) with some manipulation yields

$$M^{(2)}(s) = 1 - \frac{2sP_{SU}}{R_{32}} \times \int_{R_2}^{R_3} \frac{r dr}{\sqrt{(r^2 + (sP_{SU} - R_1^2))^2 + 4sP_{SU}R_1^2}}.$$

Applying the transformation $v = r^2$ in the above integral then gives

$$M^{(2)}(s) = 1 - \frac{sP_{SU}}{R_{32}} \times \int_{R_2^2}^{R_3^2} \frac{dv}{\sqrt{(v + (sP_{SU} - R_1^2))^2 + 4sP_{SU}R_1^2}}.$$

This integral can be solved using [33, eq. 2.261] and substituting the result back into (5) with some algebraic manipulation gives the MGF in (11). Now some trivial substitutions for R_1, R_2 and R_3 yield the MGF expressions corresponding to Case B and C.

B. Proof of Proposition 2

Following (9), the MGF corresponding to $\alpha = 4$ can be written as

$$M^{(4)}(s) = \frac{1}{\pi R_{32}} \int_{R_2}^{R_3} r g^{(4)}(r)\, dr \tag{33}$$

where

$$g^{(4)}(r) = 2\pi - 2sP_{SU} \int_0^{\pi} \frac{d\theta}{b_0(r) - b_1(r)\cos\theta + b_2(r)\cos^2\theta}$$

with $b_0(r) = \left(r^2 + R_1^2\right)^2 + sP_{SU}$, $b_1(r) = 4\left(r^2 + R_1^2\right) R_1 r$ and $b_2(r) = 4R_1^2 r^2$. Using the transformation $v = \tan(\theta/2)$ and the relation $\cos\theta = \left(\left(1 - v^2\right) / \left(1 + v^2\right)\right)$ in the above integral then yields

$$g^{(4)}(r) = 2\pi - 4sP_{SU} \int_0^{\infty} \frac{\left(1 + v^2\right) dv}{c_4(r)v^4 + 2c_2(r)v^2 + c_0(r)} \tag{34}$$

where $c_4(r) = b_0(r) + b_1(r) + b_2(r)$, $c_2(r) = b_0(r) - b_2(r)$ and $c_0(r) = b_0(r) - b_1(r) + b_2(r)$. Evaluating (34) with the help of [36, eq. 2.2.10.4] and substituting the answer back into (33) yields

$$M^{(4)}(s) = 1 - \frac{\sqrt{2}sP_{SU}}{R_{32}} \int_{R_2}^{R_3} \frac{r}{\sqrt{c_2(r) + \sqrt{c_4(r)c_0(r)}}} \times \left(\frac{1}{\sqrt{c_0(r)}} + \frac{1}{\sqrt{c_4(r)}}\right) dr.$$

Unfortunately, the above integral seems intractable for the most general spatial configuration depicted in Fig. 1 (i.e., Case A). However, we can simplify the above integral in the Case B to yield

$$M^{(4)}(s) = 1 - \frac{2sP_{SU}}{R_{32}} \int_{R_2}^{R_3} \frac{r dr}{r^4 + sP_{SU}}. \tag{35}$$

Finally, (35) can be evaluated using [33, eq. 2.132.2] which leads to the MGF given in (12) corresponding to the Case B. Again, some trivial substitutions for R_1, R_2 and R_3 yield the MGF expressions corresponding to Case C and D.

Appendix B
Proof of Proposition 3

First let us focus on obtaining the first order expansion for $\alpha = 2$ Case A. To this end, we use the substitution $z = 1/s$ in (11) to obtain

$$\mathcal{M}_I^{(2,A)}(1/z) = \exp\left(-\frac{1}{z} P_{SU}\lambda\pi \ln \frac{\mathcal{Q}(z, R_3)}{\mathcal{Q}(z, R_2)}\right) \tag{36}$$

where

$$\mathcal{Q}(z, x) = \sqrt{\frac{4R_1^2}{P_{SU}} z + \left(\frac{x^2 - R_1^2}{P_{SU}} z + 1\right)^2} + \left(\frac{x^2 - R_1^2}{P_{SU}} z + 1\right).$$

Now we can use the Taylor expansion of $\mathcal{M}_I^{(2,A)}(1/z)$ around $z = 0$ to obtain,

$$\mathcal{M}_I^{(2,A)}(1/z) \approx a_0 + a_1 z \tag{37}$$

where

$$a_0 = \lim_{z\to 0} \mathcal{M}_I^{(2,A)}(1/z) \text{ and } a_1 = \lim_{z\to 0} \frac{d}{dz}\left(\mathcal{M}_I^{(2,A)}(1/z)\right).$$

Using the L'Hôpital rule with some algebraic manipulation gives

$$a_0 = \lim_{z\to 0} \mathcal{M}_I^{(2,A)}(1/z) = \exp\left(-\lambda\pi R_{32}\right).$$

Taking the derivative of $\mathcal{M}_I^{(2,A)}(1/z)$ with respect to z yields

$$\frac{d}{dz}\left(\mathcal{M}_I^{(2,A)}(1/z)\right) = P_{SU}\lambda\pi \mathcal{M}_I^{(2,A)}(1/z) \times \left(\frac{\mathcal{Q}(z, R_3)\mathcal{Q}^{'}(z, R_2)}{z\mathcal{Q}(z, R_2)\mathcal{Q}^{(}z, R_3)} - \frac{\mathcal{Q}(z, R_2)\mathcal{Q}^{'}(z, R_3)}{z\mathcal{Q}(z, R_2)\mathcal{Q}^{(}z, R_3)} + \frac{\ln \mathcal{Q}(z, R_3) - \ln \mathcal{Q}(z, R_2)}{z^2}\right)$$

where

$$\mathcal{Q}^{'}(z, x) = \frac{x^2 - R_1^2}{P_{SU}} + \frac{\frac{2R_1^2}{P_{SU}} + \frac{x^2 - R_1^2}{P_{SU}}\left(\frac{x^2 - R_1^2}{P_{SU}} z + 1\right)}{\sqrt{\frac{4R_1^2}{P_{SU}} z + \left(\frac{x^2 - R_1^2}{P_{SU}} z + 1\right)^2}}.$$

Again, using the L'Hôpital rule gives

$$\lim_{z\to 0} \frac{d}{dz}\left(\mathcal{M}_I^{(2,A)}(1/z)\right) = P_{SU}\lambda\pi \exp\left(-\lambda\pi R_{32}\right) \times \lim_{z\to 0} \frac{\mathcal{Q}(z, R_3)\mathcal{Q}^{'}(z, R_2) - \mathcal{Q}(z, R_2)\mathcal{Q}^{'}(z, R_3)}{2z\mathcal{Q}(z, R_2)\mathcal{Q}^{(}z, R_3)}.$$

The above limit can be evaluated with the L'Hôpital rule to obtain

$$a_1 = \exp\left(-\lambda\pi R_{32}\right) \frac{\lambda\pi\left(\left(R_3^4 - R_2^4\right) + 2R_1^2 R_{32}\right)}{2P_{SU}}. \tag{38}$$

Applying the same variable transformation, $z = 1/s$, as before and using the Taylor expansions of $\arctan(R_3^2/\sqrt{sP_{SU}})$ and $\arctan(R_2^2/\sqrt{sP_{SU}})$ [33, eq. 1.643.1] in (12) yield the MGF corresponding to $\alpha = 4$ Case B as

$$\mathcal{M}_I^{(4,B)}(1/z) = \exp\left(-\lambda\pi\left\{\sum_{k=0}^{\infty} \frac{(-1)^k}{2k+1} \frac{R_3^{4k+2} - R_2^{4k+2}}{P_{SU}^k} z^k\right\}\right). \tag{39}$$

Clearly, the choice of $|z| < P_{SU}/R_4^3$ (i.e., $\Re(s) > R_3^4/P_{SU} > 0$) guarantees the convergence. Now, the first two coefficients of the power series expansion of (39) around the origin give $F_I^{(4,B)}(z)$, which concludes the proof.

Acknowledgment

The authors wish to thank the Editor and the anonymous reviewers for their careful comments that helped to improve the quality of this paper. The first author wishes to thank Dr. K. Kansanen and Dr. M. Brandt-Pearce for helpful discussions.

REFERENCES

[1] J. Mitola, "An integrated agent architecture for software defined radio," Ph.D. dissertation, Royal Institute Technology (KTH), Stockholm, Sweden, 2000.

[2] S. Haykin, "Cognitive radio: brain-empowered wireless communications," *IEEE J. Sel. Areas Commun.*, vol. 23, no. 2, pp. 201–220, Feb. 2005.

[3] E. Hossain, D. Niyato, and Z. Han, *Dynamic Spectrum Access and Management in Cognitive Radio Networks*. Cambridge University Press, 2009.

[4] A. Ghasemi and E. S. Sousa, "Interference aggregation in spectrum-sensing cognitive wireless networks," *IEEE J. Sel. Topics Signal Process.*, vol. 2, no. 1, pp. 41–56, Feb. 2008.

[5] Z. Chen, C. X. Wang, X. Hong, J. Thompson, S. A. Vorobyov, X. Ge, H. Xiao, and F. Zhao, "Aggregate interference modeling in cognitive radio networks with power and contention control," *IEEE Trans. Commun.*, vol. 60, no. 2, pp. 456–468, Feb. 2011.

[6] X. Hong, C. X. Wang, and J. Thompson, "Interference modeling of cognitive radio networks," in *Proc. 2008 IEEE VTC – Spring*, pp. 1851–1855.

[7] R. Dahama, K. W. Sowerby, and G. B. Rowe, "Outage probability estimation for licensed systems in the presence of cognitive radio interference," in *Proc. 2009 IEEE VTC – Spring*, pp. 1–5.

[8] M. Timmers, S. Pollin, A. Dejonghe, A. Bahai, L. van der Perre, and F. Catthoor, "Accumulative interference modeling for cognitive radios with distributed channel access," in *Proc. 2008 IEEE CrownCom*, pp. 1–7.

[9] M. F. Hanif, M. Shafi, P. J. Smith, and P. Dmochowski, "Interference and deployment issues for cognitive radio systems in shadowing environments," in *Proc. 2009 IEEE ICC*, pp. 1–6.

[10] E. S. Sousa and J. A. Silvester, "Optimum transmission ranges in a direct-sequence spread-spectrum multihop packet radio network," *IEEE J. Sel. Areas Commun.*, vol. 8, no. 5, pp. 762–771, June 1990.

[11] M. Souryal, B. Vojcic, and R. Pickholtz, "Ad-hoc, multihop CDMA networks with route diversity in a Rayleigh fading channel," in *Proc. 2001 IEEE MILCOM*, pp. 1003–1007.

[12] S. Singh, N. B. Mehta, A. F. Molisch, and A. Mukhopadhyay, "Moment-matched lognormal modeling of uplink interference with power control and cell selection," *IEEE Trans. Wireless Commun.*, vol. 9, no. 3, pp. 932–938, Mar. 2010.

[13] M. Aljuaid and H. Yanikomeroglu, "A cumulant-based characterization of the aggregate interference power in wireless networks," in *Proc. 2010 IEEE VTC – Spring*, pp. 1–5.

[14] M. Z. Win, P. C. Pinto, and L. A. Shepp, "A mathematical theory of network interference and its applications," *Proc. IEEE*, vol. 97, no. 2, pp. 1–26, Feb. 2009.

[15] R. Menon, R. M. Buehrer, and J. H. Reed, "On the impact of dynamic spectrum sharing techniques on legacy radio systems," *IEEE Trans. Wireless Commun.*, vol. 7, no. 11, pp. 4198–4207, Nov. 2008.

[16] S. Srinivasa and M. Haenggi, "Modeling interference in finite uniformly random networks," in *Proc. 2007 Int. Workshop Inf. Theory Sensor Netw.*

[17] E. Salbaroli and A. Zanella, "Interference analysis in a Poisson field of nodes of finite area," *IEEE Trans. Veh. Technol.*, vol. 58, no. 4, pp. 1776–1783, May 2009.

[18] M. Vu and V. Tarokh, "On the primary exclusive region of cognitive networks," *IEEE Trans. Wireless Commun.*, vol. 8, no. 7, pp. 3380–3385, July 2009.

[19] A. Hasan and J. G. Andrews, "The guard zone in wireless ad hoc networks," *IEEE Trans. Commun.*, vol. 6, no. 3, pp. 897–906, Mar. 2007.

[20] C. Cordeiro, K. Challapali, D. Birru, and S. Shankar, "IEEE 802.22: an introduction to the first wireless standard based on cognitive radios," *J. Commun.*, vol. 1, no. 1, pp. 38–47, Apr. 2006.

[21] J. D. Parsons, *The Mobile Radio Propagation Channel*, 2nd edition. Wiley, 2000.

[22] H. S. Dhillon, R. K. Ganti, and J. G. Andrews, "A tractable framework for coverage and outage in heterogeneous cellular networks," in *Proc. 2011 IEEE Inf. Theory Applications Workshop*, pp. 1–6.

[23] S. Srinivasa and M. Haenggi, "Distance distributions in finite uniformly random networks: theory and applications," *IEEE Trans. Veh. Technol.*, vol. 59, no. 2, pp. 940–949, Feb. 2010.

[24] J. G. Andrews, R. K. Ganti, M. Haenggi, N. Jindal, and S. Weber, "A primer on spatial modeling and analysis in wireless networks," *IEEE Commun. Mag.*, vol. 48, no. 11, pp. 156–163, Nov. 2010.

[25] G. L. Stüber, *Principles of Mobile Communication*, 2nd edition. Kluwer Academic Publishers, 2001.

[26] A. Papoulis and S. U. Pillai, *Probability, Random Variables and Stochastic Processes*, 4th edition. McGraw Hill, 2002.

[27] H. Inaltekin, M. Chiang, H. V. Poor, and S. B. Wicker, "On unbounded path-loss models: effects of singularity on wireless network performance," *IEEE J. Sel. Areas Commun.*, vol. 27, no. 7, pp. 1078–1092, Sep. 2009.

[28] A. Rabbachin, T. Q. S. Quek, S. Hyundong, and M. Z. Win, "Cognitive network interference," *IEEE J. Sel. Areas Commun.*, vol. 29, no. 2, pp. 480–493, Feb. 2011.

[29] A. P. Prudnikov, Y. A. Brychkov, and O. I. Marichev, *Integral and Series, Volume 5: Inverse Laplace Transforms*. Gordon and Breach Science Publishers, 1992.

[30] A. M. Mathai and S. B. Provost, *Quadratic Forms in Random Variables*. Marcel Dekker, 1992.

[31] J. Abate and W. Whitt, "The Fourier-series method for inverting transforms of probability distributions," *Queueing Syst.*, vol. 10, pp. 5–88, 1992.

[32] M. K. Simon and M. S. Alouini, *Digital Communication over Fading Channels*, 2nd edition. Wiley, 2005.

[33] I. S. Gradshteyn and I. M. Ryzhik, *Tables of Integrals, Series and Products*. Academic Press, 1980.

[34] L. Xiao and X. Dong, "Error performance of orthogonal signaling family in Ricean-fading channels with maximal ratio combining," *IEEE Trans. Veh. Technol.*, vol. 53, no. 6, pp. 1942–1947, Nov. 2004.

[35] Z. Wang and G. B. Giannakis, "A simple and general parametrization quantifying performance in fading channels," *IEEE Trans. Commun.*, vol. 51, no. 8, pp. 1389–1398, Aug. 2003.

[36] A. P. Prudnikov, Y. A. Brychkov, and O. I. Marichev, *Integrals and Series: Elementary Functions*. Gordon and Breach Science Publishers, 1986.

Luxmiram Vijayandran (S'08) received his diplôme d'ingénieur at EFREI, Grandes Ecoles, France, and the M.Sc. degree at CHALMERS, Sweden, in 2005 and 2006, respectively. He is in the process of completing his Ph.D. in the Department of Electronics and Telecommunications at the Norwegian University of Science and Technology (NTNU) in Trondheim, Norway, in 2012. Since November 2011, he has been with Thales Communication and Security in France, conducting research on MAC layer and physical layer issues. Before becoming a Ph.D. candidate, he was with EADS Telecom and Thales in France from January 2006 to May 2008. His research interests include optimization, estimation theory, control theory, queueing theory, and cognitive radio in general.

Prathapasinghe Dharmawansa (S'05-M'09) received the B.Sc. and M.Sc. degrees in electronic and telecommunication engineering from the University of Moratuwa, Moratuwa, Sri Lanka, in 2003 and 2004, respectively, and the D.Eng. degree in information and communications technology from the Asian Institute of Technology, Thailand, in 2007. He subsequently joined the Department of Electronic and Computer Engineering, Hong Kong University of Science and Technology (HKUST), as a Research Associate. Since October 2011, he has been with the Department of Communications and Networking, Aalto University School of Electrical Engineering, Finland, as a Postdoctoral Researcher. His research interests are in communications and signal processing, random matrix theory, and multivariate statistics. He received the Best Paper Award in Communication Theory at the IEEE International Conference on Communications (ICC 2011) held in Kyoto, Japan.

Torbjörn Ekman was born in Västerås, Sweden, in 1969. He received the M.Sc. degree in engineering physics in 1994 and the Ph.D. degree in signal processing in 2002, both from Uppsala University, Sweden. In 2006, he joined the Department of Electronics and Telecommunications at the Norwegian University of Science and Technology (NTNU) in Trondheim, Norway, as an Associate Professor. From 1997 to 1998, he was a visiting scientist at the Institute of Communications and Radio-Frequency Engineering, Vienna University of Technology, Vienna, Austria, on a Marie Curie Grant. From 1999 to 2002, he was visiting the Digital Signal Processing Group, University of Oslo, Norway. In 2002–2005, he made his postdoctoral studies at UniK, University Graduate Center, Kjeller, Norway. His current research interests include signal processing in wireless communications, scheduling of radio resources and dynamic modeling, and prediction of radio channels. He is currently participating in projects on broadband radio access and cognitive radio, studying radio resource management and channel modeling.

Chintha Tellambura (F'11) received the B.Sc. degree (with first-class honor) from the University of Moratuwa, Sri Lanka, in 1986, the M.Sc. degree in electronics from the University of London, U.K., in 1988, and the Ph.D. degree in electrical engineering from the University of Victoria, Canada, in 1993. He was a Postdoctoral Research Fellow with the University of Victoria (1993–1994) and the University of Bradford (1995–1996). He was with Monash University, Australia, from 1997 to 2002. Presently, he is a Professor with the Department of Electrical and Computer Engineering, University of Alberta. His research interests focus on communication theory dealing with the wireless physical layer. Prof. Tellambura is an Associate Editor for the IEEE TRANSACTIONS ON COMMUNICATIONS and the Area Editor for Wireless Communications Systems and Theory in the IEEE TRANSACTIONS ON WIRELESS COMMUNICATIONS. He was Chair of the Communication Theory Symposium in Globecom'05 held in St. Louis, MO.